Nyquist-shaped dispersion-precompensated subcarrier modulation with direct detection for spectrally-efficient WDM transmission

M. S. Erkılınç,[1,*] S. Kilmurray,[1] R. Maher,[1] M. Paskov,[1] R. Bouziane,[1] S. Pachnicke,[2] H. Griesser,[3] B. C. Thomsen,[1] P. Bayvel[1] and R. I. Killey[1]

[1]*Optical Networks Group, Dept. of Electronic & Electrical Engineering, University College London, Torrington Place, London, WC1E 7JE, UK*
[2]*ADVA Optical Networking SE, Maerzenquelle 1-3, 98617 Meiningen, Germany*
[3]*ADVA Optical Networking SE, Fraunhoferstr. 9a, 82152 Martinsried, Germany*
**m.erkilinc@ee.ucl.ac.uk*

Abstract: The use of single-sideband subcarrier modulation (SCM) with Nyquist (N) pulse shaping for cost-effective spectrally-efficient wavelength division multiplexed transmission with direct detection is described. Transmission of digitally pre-compensated 7 × 11 GHz-spaced N-QPSK SCM channels at 14 Gb/s per channel is experimentally demonstrated over distances of up to 800 km of uncompensated standard single-mode fiber (SSMF) (13440 ps/nm chromatic dispersion).

OCIS codes: (060.0060) Fiber optics and optical communications; (060.2360) Fiber optics links and subsystems.

References and links

1. J. Barry, *Wireless Infrared Communications*, Kluwer Academic Publishers, Norwell, MA, USA, 1994.
2. T. Ohtsuki, "Multiple-subcarrier modulation in optical wireless communications," IEEE Commun. Magazine **41**, 74–79 (2003).
3. R. Hui, B. Zhu, R. Huang, C. Allen, K. Demarest, and D. Richards, "10-Gb/s SCM fiber system using optical SSB modulation," IEEE Photon. Tech. Lett. **13**, 896–898 (2001).
4. A. J. Lowery and L. B. Du, "Optical orthogonal division multiplexing for long haul optical communications: A review of the first five years," Optical Fiber Tech. **17**, 421–438 (2011).
5. J. Armstrong, "OFDM for optical communications," J. Lightwave Technol. **27**, 189–204 (2009).
6. J. Kahn and J. Barry, "Wireless infrared communications," Proc. of the IEEE **85**, 265–298 (1997).
7. A. O. Wiberg, B.-E. Olsson, and P. A. Andrekson, "Single cycle subcarrier modulation," in *Optical Fiber Communication Conference*, OSA Technical Digest, (2009), paper OTuE1.
8. B.-E. Olsson and A. Alping, "Electro-optical subcarrier modulation transmitter for 100 GbE DWDM transport," in *Asia Optical Fiber Communication and Optoelectronic Exposition and Conference,* OSA Technical Digest, (2008), paper SaF3.
9. T.-T. Pham, R. Rodes, J. B. Jensen, C. J. Chang-Hasnain, and I. T. Monroy, "Sub-cycle QAM modulation for VCSEL-based optical fiber links," Opt. Express **21**, 1830–1839 (2013).
10. A. S. Karar and J. C. Cartledge, "Generation and detection of a 56 Gb/s signal using a DML and half-cycle 16-QAM Nyquist-SCM," IEEE Photon. Tech. Lett. **25**, 757–760 (2013).
11. G. Bosco, A. Carena, V. Curri, P. Poggiolini, and F. Forghieri, "Performance Limits of Nyquist-WDM and CO-OFDM in High-Speed PM-QPSK Systems," IEEE Photon. Tech. Lett. **22**, 1129-1131 (2010).
12. M. Erkilinc, R. Maher, M. Paskov, S. Kilmurray, S. Pachnicke, H. Griesser, B. Thomsen, P. Bayvel, and R. Killey, "Spectrally-efficient single-sideband subcarrier-multiplexed quasi-Nyquist QPSK with direct detection," in *European Conference and Exhibition on Optical Communication,* (2013), paper Tu3C4.
13. W. Rosenkranz and C. Xia, "Electrical equalization for advanced optical communication systems," AEU-Int. J. of Electron. and Commun. **61**, 153–157 (2007).
14. H. Bülow, F. Buchali, and A. Klekamp, "Electronic dispersion compensation," J. Lightwave Technol. **26**, 158–167 (2008).

#201923 - $15.00 USD Received 28 Nov 2013; revised 6 Feb 2014; accepted 13 Mar 2014; published 11 Apr 2014

15. G. Katz and D. Sadot, "A nonlinear electrical equalizer with decision feedback for OOK optical communication systems," IEEE Trans. on Commun. **56**, 2002–2006 (2008).
16. Q. Yu, "On the decision-feedback equalizer in optically amplified direct-detection systems," J. Lightwave Technol. **25**, 2090–2097 (2007).
17. M. Cavallari, C. Fludger, and P. Anslow, "Electronic signal processing for differential phase modulation formats," in *Optical Fiber Communication Conference,* OSA Technical Digest, (2004), paper TuG2.
18. O. E. Agazzi, M. R. Hueda, H. S. Carrer, and D. E. Crivelli, "Maximum-likelihood sequence estimation in dispersive optical channels," J. Lightwave Technol. **23**, 749 (2005).
19. T.L. Koch, and R.C. Alferness, "Dispersion compensation by active predistorted signal synthesis," J. Lightwave Technol. **LT-3**, 800–805 (1985).
20. R. I. Killey, P. M. Watts, V. Mikhailov, M. Glick, and P. Bayvel, "Electronic dispersion compensation by signal predistortion using digital processing and a dual-drive Mach-Zehnder modulator," IEEE Photon. Tech. Lett. **17**, 714–716 (2005).
21. J. McNicol, M. O'Sullivan, K. Roberts, A. Comeau, D. McGhan, and L. Strawczynski, "Electrical domain compensation of optical dispersion [optical fibre communication applications]," in *Optical Fiber Communication Conference,* OSA Technical Digest, (2005), paper OThJ3.
22. M. M. El Said, J. Sitch, and M. I. Elmasry, "An electrically pre-equalized 10-Gb/s duobinary transmission system," J. Lightwave Technol. **23**, 388 (2005).
23. M. Erkilinc, S. Kilmurray, S. Pachnicke, H. Griesser, B. Thomsen, P. Bayvel, and R. Killey, "Nyquist-Shaped Dispersion-Precompensated Subcarrier Modulation with Direct Detection," in *Optical Fiber Communication Conference,* (2014), paper Th3K4.
24. F. Chang, K. Onohara and T. Mizuochi, "Forward error correction for 100 G transport networks," IEEE Commun. Magazine, **48**, S48–S55 (2010).
25. G. P. Agrawal, *Applications of nonlinear fiber optics*, 3rd ed., Academic press, 2010.
26. R. A. Shafik, S. Rahman, R. Islam, and N. S. Ashraf, "On the error vector magnitude as a performance metric and comparative analysis," in *2nd Int'l. Conference on Emerging Technologies,* (2006).

1. Introduction

The demand for higher bit rate transmission using cost-effective solutions is continuously increasing in metro, access and back-haul optical communication systems. Consequently, there is significant interest in the use of high-order modulation techniques to meet this demand, where the data is encoded using both optical phase and amplitude modulation. The most spectrally efficient systems employ coherent receivers. However, direct detection systems may provide a more cost-effective solution for short and medium distance links due to the lower the number of optical components required, *i.e.,* no optical hybrids, local oscillator laser, polarization beam combiner/splitter and balanced detectors. Moreover, the lower complexity of digital signal processing (DSP) at the receiver avoids the need for polarization tracking, frequency offset estimation and carrier phase estimation and allows the use of larger linewidth (and hence lower cost) lasers. Thus, new approaches to increase the spectral efficiency of direct detection systems need to be explored.

In the simple direct-detected system architecture considered in this paper (see Fig. 1), if a single photodetector with no delay interferometers is used in each receiver, the optical phase of the signal is lost upon photodetection. However, the data can be modulated on one or more RF-subcarriers [1–3], utilizing the subcarrier modulation (SCM) technique. Using this technique allows the amplitude and phase of each subcarrier to be recovered after detection, since the subcarrier beats with the optical carrier within the bandwidth of the photodetector. A spectrally-efficient example of multiple-subcarrier modulation (MSM) is orthogonal frequency division multiplexing (OFDM) [4]. The main disadvantage of OFDM signaling is the high peak-to-average power ratio (PAPR) since the relative phases of the subcarriers can add constructively, leading to high peaks in time domain signal. This causes a degradation in receiver sensitivity. Signal clipping can be used to reduce the PAPR, although this results in nonlinear distortion and penalties. Other techniques for reducing the PAPR for OFDM have been investigated, though all have increased complexity or overheads [4, 5].

Alternatively, single subcarrier modulation, introduced in wireless infrared and optical com-

#201923 - $15.00 USD Received 28 Nov 2013; revised 6 Feb 2014; accepted 13 Mar 2014; published 11 Apr 2014

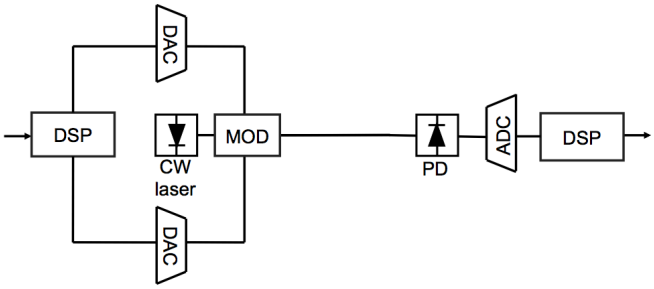

(a)

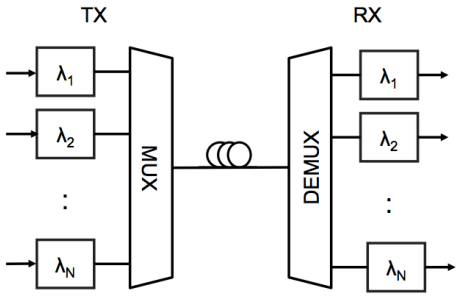

(b)

Fig. 1. System architecture (a) transceiver design and (b) WDM transmission system. DSP: Digital signal processing, DAC: Digital-to-analogue converter, CW: Continous wave, MOD: Modulator, PD: Photodiode, ADC: Analogue-to-digital converter, TX: Transmitter, MUX: Multiplexer, DEMUX: Demultiplexer and RX: Receiver.

munication [1, Ch. 5] [6], can be used for higher-order modulation with direct detection. In this method, the data is first electrically modulated onto a single RF-subcarrier by applying conventional quadrature amplitude modulation (QAM) with a direct current (DC) bias to avoid clipping and then converted to an optical signal. The lower PAPR compared to OFDM signaling potentially improves system performance.

The choice of the subcarrier frequency (f_{sc}) determines the optical spectral efficiency. Its value should be selected to be as close as possible to the optical carrier to maximize the spectral efficiency. Single-cycle quaternary phase-shift keying (QPSK) and 16-QAM SCM, in which the subcarrier frequency is set equal to the symbol rate (f_b), was investigated in [7, 8]. To further increase the spectral efficiency, half-cycle subcarrier modulation, with and without Nyquist pulse shaping, were demonstrated back-to-back and in transmission over VCSEL-based short optical links (up to 20 km) in [9, 10]. A description of Nyquist pulse shaping can be found in [11]. The frequency difference between the optical carrier and the subcarrier is just half of the symbol rate, so that the spectral efficiency becomes $(\log_2(M))/2$ for half-cycle M-QAM SCM signals. The single- and half-cycle concepts are depicted in Fig. 2(a) and 2(b).

However, a further increase in optical spectral efficiency can be achieved using single-sideband (SSB) SCM signalling. One of the sidebands can be eliminated by applying a digital sideband filter in the transmitter, if a vector modulator (e.g. an IQ-modulator [12] or dual-drive Mach-Zehnder modulator) is used. Hence, in this paper, we demonstrate the generation, transmission and detection of SSB SCM with Nyquist pulse shaping as shown schematically in Fig. 2(c).

In addition to high spectral efficiency, another desirable feature of a transceiver is tolerance

#201923 - $15.00 USD Received 28 Nov 2013; revised 6 Feb 2014; accepted 13 Mar 2014; published 11 Apr 2014

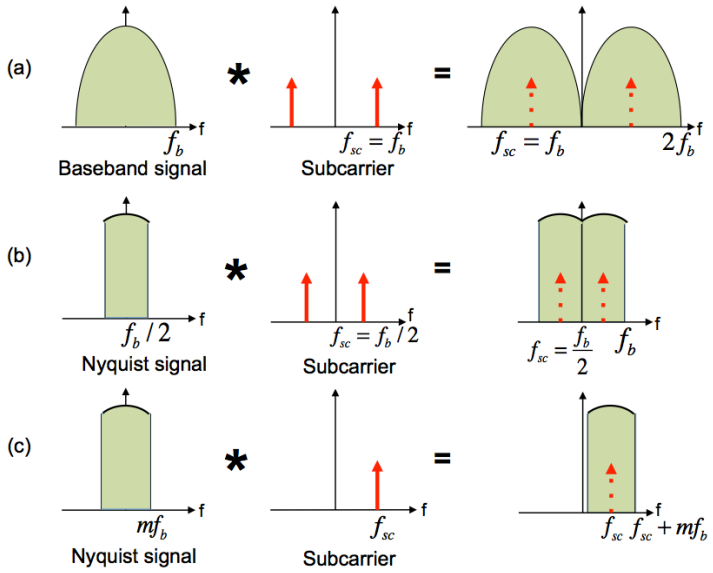

Fig. 2. Schematics of signal spectra. (a) DSB single-cycle SCM, (b) DSB half-cycle SCM, and (c) SSB fractional cycle ($0.5 \leqslant f_{sc}/f_b \leqslant 1$) Nyquist ($0.5 \leqslant m \leqslant 1$) SCM. ($f_{sc}$ and f_b are the subcarrier frequency and symbol rate, respectively.)

to chromatic dispersion. The effect of chromatic dispersion in direct detection systems is transformed from a linear distortion in the optical domain to a non-linear distortion in the electrical domain by square-law detection. Significant penalties remain after receiver-based equalization and the complexity of nonlinear equalization such as maximum likelihood sequence estimation (MLSE) increases exponentially with the dispersion accumulated along the fiber [13–18]. Therefore, electronic pre-dispersion (EPD) compensation, proposed in [19–22], is used as an alternative method in which the chromatic dispersion can be compensated at the transmitter by pre-distorting the signal with the inverse of the channel response.

In [12], we proposed, for the first time, single-sideband QPSK subcarrier modulation with Nyquist pulse shaping and investigated its back-to-back performance for single channel and wavelength division multiplexing (WDM) direct-detected systems. Single channel transmission of Nyquist-QPSK SCM over 800 km of SSMF utilizing EPD was experimentally demonstrated in [23]. Here, we present, for the first time, a numerical and experimental study of WDM transmission using Nyquist pulse-shaped dispersion-precompensated QPSK SCM with direct detection. To show the effectiveness of this technique, we carried out transmission experiments with 7-channel 11 GHz-spaced WDM signals over distances of up to 800 km of uncompensated SSMF (13440 ps/nm chromatic dispersion). Transmission at a bit rate of 14 Gb/s per channel with spectral efficiency of 1.3 b/s/Hz (1.2 b/s/Hz assuming a 7 % hard decision forward error correction (HD-FEC) overhead) [24] was achieved.

2. Parameter optimization and numerical simulations

In this section, simulation principles and numerical simulations that were carried out to optimize the transmitter characteristics in order to achieve high spectral efficiency with low required optical signal-to-noise ratio (OSNR) are described. A high spectral efficiency, (approaching $\log_2(M)$ b/s/Hz for M-QAM), can be achieved by using SSB SCM with Nyquist pulse-shaping using root raised cosine filters (RRCs) with a roll-off factor (α) of 0. However, this roll-off

#201923 - $15.00 USD Received 28 Nov 2013; revised 6 Feb 2014; accepted 13 Mar 2014; published 11 Apr 2014

factor causes high PAPR which leads to a degradation in receiver sensitivity caused by digital-to-analogue converter (DAC) quantization noise and the requirement for high optical carrier power to maintain a unipolar signal at the receiver (essential for direct detection). Therefore, a value of α greater than zero can be used to achieve a trade-off between the spectral efficiency and the required OSNR.

In order to choose the value of α and corresponding subcarrier frequency, the proposed direct-detected system was first studied by means of numerical simulations, using MATLAB. Single side-band Nyquist-spaced QPSK SCM signals at a bit rate of 14 Gb/s (a symbol rate (f_b) of 7 GBaud) were generated using DACs operating at 28 GSa/s with 6-bit nominal resolution (with an effective number of bits (ENOB) of 3.6 at 10 GHz). The variations of the PAPR versus roll-off factor (α) for a variety of subcarrier frequencies (f_{sc}) are plotted in Fig. 3(a) whilst the required OSNR values (with 0.1 nm resolution bandwidth) at the HD-FEC limit, taken to be 3.8×10^{-3}, are plotted in Fig. 3(b) with a subcarrier frequency of $0.75f_b$ (5.25 GHz). The signal bandwidth (the bandwidth between the optical carrier and the frequency at which the signal power drops to zero, assuming ideal RRC pulse shaping filter) versus roll-off factor is also plotted in Fig. 3(c). It can be seen that both the PAPR and required OSNR decrease with increasing roll-off factor from 0 to 0.4 whilst the bandwidth of the signal is increasing. Beyond this point, the change in both PAPR and the required OSNR is less significant.

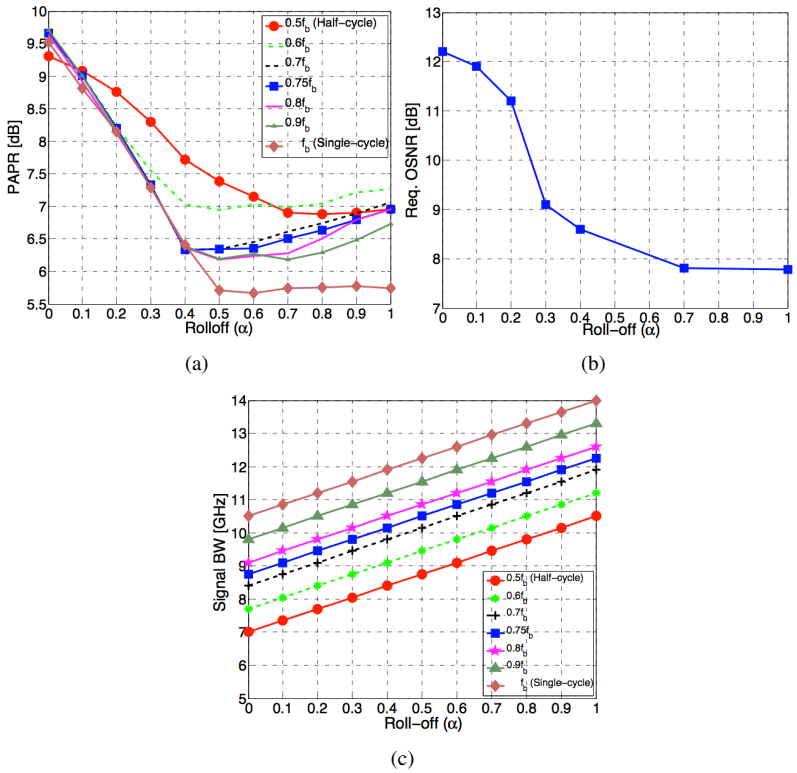

Fig. 3. (a) PAPR versus α for different subcarrier frequencies. (b) Required OSNR versus α with $f_{sc}=0.75f_b$ at the HD-FEC limit including the DAC quantization noise. (c) Signal bandwidth vs α for different subcarrier frequencies.

Based on these simulations, a roll-off factor of 0.3 with a subcarrier frequency of 5.25 GHz, (and hence signal bandwidth of 9.8 GHz ($0.75\,f_b+f_b/2+f_b\,\alpha/2$) as shown in Fig. 3(c)) was selected to achieve a good trade-off between the spectral efficiency and required OSNR for our

#201923 - $15.00 USD Received 28 Nov 2013; revised 6 Feb 2014; accepted 13 Mar 2014; published 11 Apr 2014

experimental demonstration.

Transmission simulations using a simulation tool developed in MATLAB within the group based on the solution of nonlinear Schrdinger equation (NLSE) with ideal conditions and practical parameters were performed over different distances with the chosen values of f_{sc} and α. All 7 WDM channels with a channel spacing of 11 GHz carrying 14 Gb/s single-sideband N-QPSK subcarrier modulated signal were decorrelated by 0.14 of the pattern length. After bit to symbol mapping using 4 samples/symbol, a pair of RRC filters with 128 taps and a roll-off factor of 0.3 were used for pulse shaping. EPD was applied to the modulated up-converted signal to pre-compensate the dispersion in frequency domain with the targeted amount of chromatic dispersion. First, no DAC quantization noise or electrical bandwidth limitation was taken into account to demonstrate the fundamental limits of the proposed transceiver. Then, simulations were performed with the practical parameters similar to the experiment, *i.e.,* ENOB at 10 GHz was set to 3.6 bits and the bandwidth limitations both at the transmitter and receiver were emulated with a 5^{th}-order Bessel low-pass with a bandwidth of 7 and 16 GHz, respectively. Besides this, IQ-modulators were assumed to be linear. The transmission link considered in the simulations was uncompensated SSMF and the fiber parameters α, D, γ, erbium-doped fiber amplifier (EDFA) noise figure and span length were chosen as 0.2 dB/km, 16.8 ps/(nmkm), 1.2 $\text{W}^{-1}\text{km}^{-1}$, 4.5 dB and 80 km, respectively. Additionally, the EDFAs were set to operate in saturation with a fixed output power of 18 dBm. The signal transmission in the fiber was modelled with the symmetrical split-step Fourier method [25] with a step size of 500 m. An ideal rectangular optical filter to simulate the ideal system and 3^{rd}-order super-Gaussian optical filter to emulate the experiment were used to demultiplex the central WDM channel. Then, it was detected by a single-ended photodiode with a responsivity of 0.9 A/W. The resolution of analogue-to-digital converter (ADC) was assumed to be infinite. Subsequent DSP consists of down-conversion, matched filter and symbol to bit mapping. Finally, as performance metrics, error vector magnitude (EVM) was measured as described in [26] and bit-error-ratio (BER) was computed by error counting. The simulation results for ideal and practical system design are discussed in Section 4.

3. Experimental transmission setup

The optical transmission test-bed used for the transmission experiments is shown in Fig. 4. It consists of a 7 x 14 Gb/s channel SSB Nyquist-QPSK SCM transmitter, an optical fiber recirculating loop and a direct detection receiver used to recover the central WDM channel. An external cavity laser (ECL) with a linewidth of 100 kHz at 1553 nm was used as a laser source for the optical comb generator (OCG in Fig. 4), which employed an optical intensity and an optical phase modulator, overdriven with an 11 GHz clock signal to generate 7×11 GHz spaced unmodulated optical channels (the channel spacing was limited by the bandwidth of the RF amplifiers used in the OCG). Kylia interleavers were used to allow separate data encoding for odd and even channels.

The block diagram of the transmitter DSP to generate the electrical driving signals (in-phase (I) and quadrature (Q) components) is shown in Fig. 5(a). The transmitter DSP was carried out offline using MATLAB before uploading the waveforms to field-programmable gate arrays (FPGAs) read-only access memory (RAM). First, a 14 Gb/s conventional QPSK signal was generated using two 2^{15} de Bruijn bit sequences de-correlated by 0.25 of the pattern length. 128-tap RRC pulse-shaping filters with a roll-off factor of 0.3 and a stop-band attenuation of 40 dB were applied to both I and Q components to achieve the Nyquist shaping. Following this, the pulse-shaped signal was up-converted by the RF-subcarrier with a frequency of 5.25 GHz ($f_{sc} = 0.75 \times f_b$) as shown in Fig. 5(a). After I and Q components were added, one of the sidebands was filtered out digitally utilizing a sideband filter. To mitigate chromatic dispersion

#201923 - $15.00 USD Received 28 Nov 2013; revised 6 Feb 2014; accepted 13 Mar 2014; published 11 Apr 2014

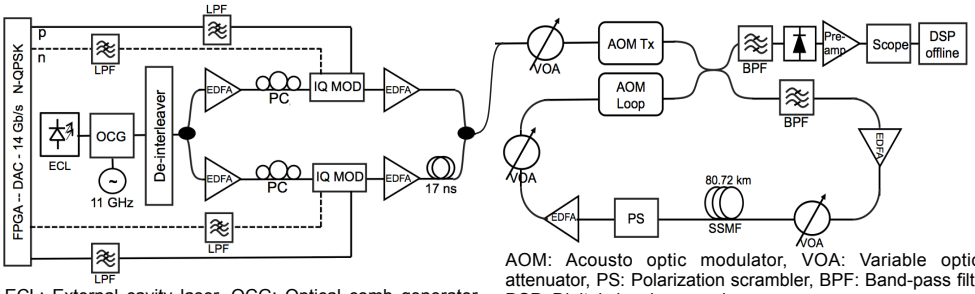

ECL: External cavity laser, OCG: Optical comb generator, DAC: Digital-to-analog converter, LPF: Low-pass filter, EDFA: Erbium-doped fiber amplifier, PC: Polarization controller.

AOM: Acousto optic modulator, VOA: Variable optical attenuator, PS: Polarization scrambler, BPF: Band-pass filter, DSP: Digital signal processing

Fig. 4. Experimental setup to demonstrate WDM SSB Nyquist-QPSK SCM transmission.

accumulated during the fiber transmission, the signal was pre-distorted by applying the EPD technique, as described in [20–22]. The relation used to pre-distort the signal at the transmitter is

$$H^{-1}(L,\omega_c) = \exp\left(-j\frac{D_{SMF}}{4\pi c_0}\lambda_o^2\omega_c^2 L\right) \tag{1}$$

where λ_0 is the carrier wavelength, c_0 is the speed of the light in vacuum, D_{SMF} is the dispersion parameter at wavelength λ_0, ω_c is the angular frequency and L is the length of the full transmission link. Finally, the waveforms were quantized to 6 bits for the DACs (Micram VEGA DACII) and uploaded to the memories of a pair of Xilinx Virtex 5 FPGAs driving the I and Q DACs.

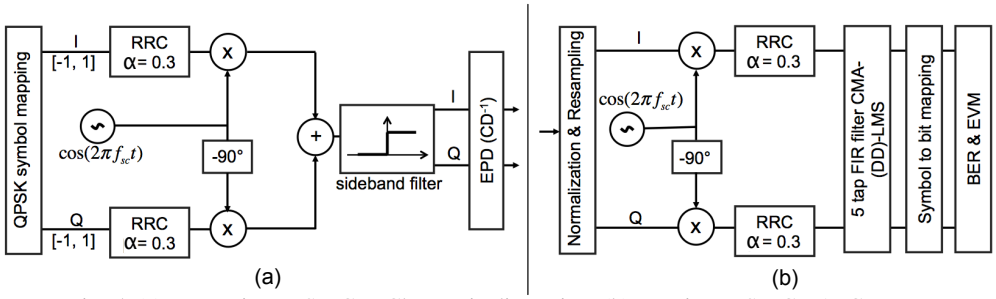

Fig. 5. (a) Transmitter DSP. CD: Chromatic dispersion. (b) Receiver DSP. CMA: Constant modulus algorithm, DD: Decision-directed LMS: Least mean squares.

Electrical anti-imaging filters (5^{th}-order Bessel low-pass filter with a bandwidth of 7 GHz) were used to avoid any crosstalk between WDM channels due to images generated by the DACs. The optical carrier was added to the modulated signal using the IQ-modulator. The modulators were operated at the quadrature point to map the electrical signals linearly to the optical domain. The odd and even channels were amplified, and coupled with a decorrelation fiber of 17 ns (approximately 150 samples) on one arm to obtain the 11 GHz spaced WDM signal for transmission. Experimental and simulated single channel optical intensity waveforms with practical parameters are shown side by side in Fig. 6 (previously shown in [12]). It indicates that there is a good agreement between the practical simulations and experiment. In one symbol period (140 ps), three-quarters of a RF-subcarrier (sine wave) with its four phases can be observed.

#201923 - $15.00 USD Received 28 Nov 2013; revised 6 Feb 2014; accepted 13 Mar 2014; published 11 Apr 2014

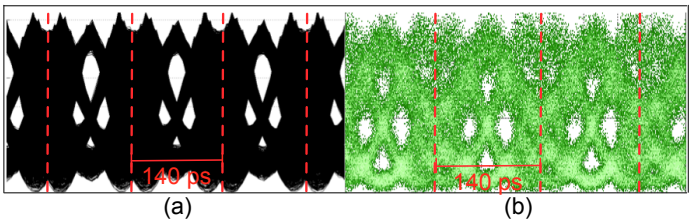

Fig. 6. (a) Simulated and (b) experimental optical intensity waveforms [12].

A recirculating optical fiber loop test-bed was used to investigate the transmission performance over cascaded spans of 80 km SSMF (D_{SMF}=16.8 ps/nm/km), as shown in Fig. 4. The loop was gated with two acousto-optic modulators (AOMs) to switch between 'signal loading from TX' and 'signal recirculation' stage. To reject the out-of-band amplified spontaneous emission (ASE) noise, a band-pass filter was utilized. Variable optical attenuators were used to control the launch power into the span and balance the loop. A loop synchronous polarization scrambler (PS) was used to scramble/randomize the state of polarization in the loop. The losses occurring due to the fiber, VOAs, PS, AOMs and filters were compensated by EDFAs with a noise figure of 4.5 dB, which were operated at the saturation point (18 dBm output power).

A tunable filter with an adjustable bandwidth (a minimum value of 4 GHz) and a filter edge gradient of 800 dB/nm (Yenista Optics XTM50-Ultrafine) was used to select the central WDM channel emulating the operation of the wavelength demultiplexer. The center frequency of ∼193.12 THz (∼5 GHz offset from the optical carrier) and 3dB bandwidth of the filter (10.5 GHz) were tuned manually to optimize the system performance. The demultiplexed signal was detected by a single-ended PIN photodiode followed by a linear amplifier, and digitized using a single ADC (Tektronix DPO 72004 oscilloscope) operating at 50 GSa/s with an electrical bandwidth of 16 GHz and a nominal resolution of 8 bits (ENOB of 5 bits at 10 GHz). The received signal was first normalized, resampled to 2 Sa/sym and down-converted to baseband as shown in Fig. 5(b). A matched filter (a RRC with a roll-off factor $\alpha = 0.3$) was subsequently applied. For clock recovery, initially, a 5-tap CMA-LMS equalizer was used for fast convergence and then switched to decision directed mode LMS. Finally, the BER was calculated by error counting, using 2^{17} symbols.

4. Transmission results and discussion

Measurements of the BER versus the received OSNR values for the central WDM channel with noise loading at the receiver were carried out to test the back-to-back and transmission performance of the system. As the central WDM channel gives the worst performance due the fiber nonlinearity compared to the other channels, the results for the central channel are presented and discussed throughout the paper. The optical spectrum of a single channel is shown in Fig. 7(a) and WDM signal before and after filtering are shown in Fig. 7(b). After filtering, the neighbouring channels were suppressed by more than 20 dB which was sufficient to recover the transmitted signal. The back-to-back received constellations and electrical spectra for the single channel and WDM case are shown in Fig. 7(c)–7(f).

The implementation penalty for the single channel case was found to be 0.8 dB compared to the simulation back-to-back case as plotted in Fig. 8. This is because of the DAC quantization noise. In the WDM back-to-back case, no penalty would be observed, if the demultiplexing was performed using an ideal rectangular filter. However, the non-ideal demultiplexing with narrow WDM spacing caused a 3.2 dB increase in EVM (the ratio of EVMs of Fig. 7(c) and 7(d)). Therefore, the distortion due to crosstalk caused an additional 1 dB required OSNR penalty at a BER of 3.8×10^{-3} compared to the experimental single channel case as shown in Fig. 8.

#201923 - $15.00 USD Received 28 Nov 2013; revised 6 Feb 2014; accepted 13 Mar 2014; published 11 Apr 2014

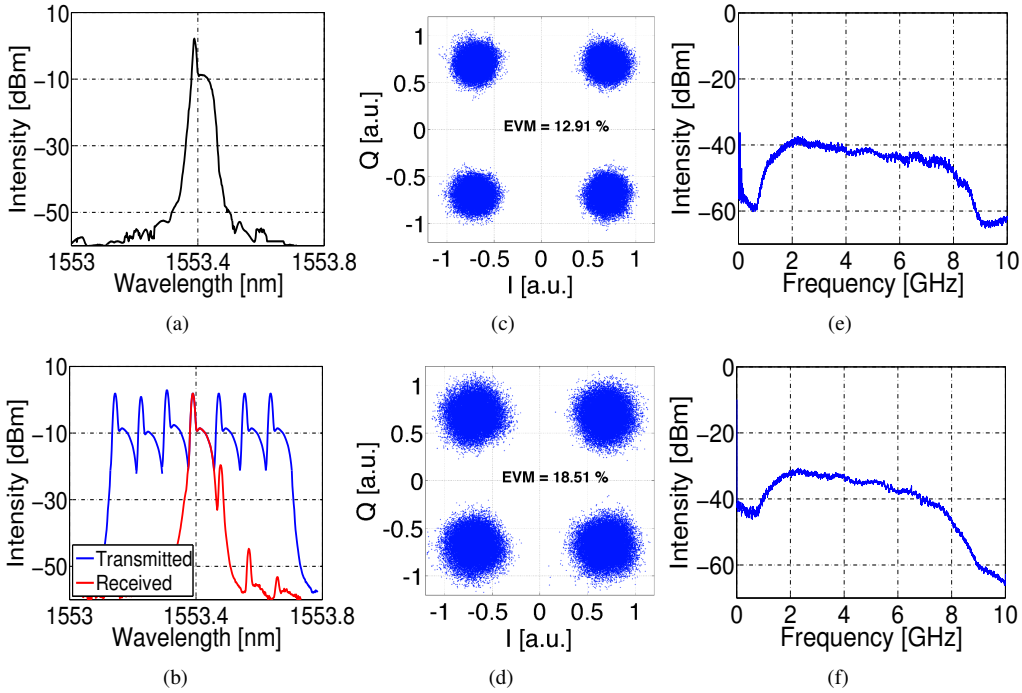

Fig. 7. Optical spectra for (a) single channel and (b) WDM system. Back-to-back received (c) single channel and (d) central WDM channel constellations. Back-to-back received electrical spectra for (e) single channel and (f) central WDM channel.

The transmission performance for both the single channel and WDM system was investigated after propagating over 400 km (5 spans) and 800 km (10 spans) of SSMF, which are typical distances for regional and long-haul applications. Although the optimum carrier-to-signal power

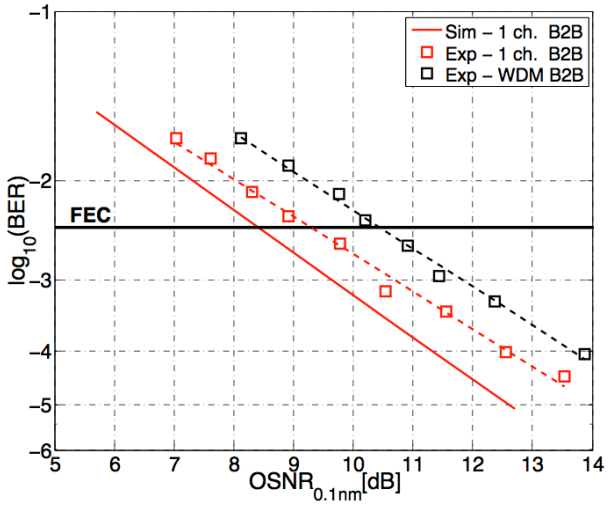

Fig. 8. Back-to-back (B2B) BER versus OSNR curves for single channel with no DAC quantization noise in simulation, single channel experiment and 7 channel experiment.

ratio (CSPR) was found to be -1 dB in the back-to-back characterization at an OSNR of 9 dB, it

#201923 - $15.00 USD Received 28 Nov 2013; revised 6 Feb 2014; accepted 13 Mar 2014; published 11 Apr 2014

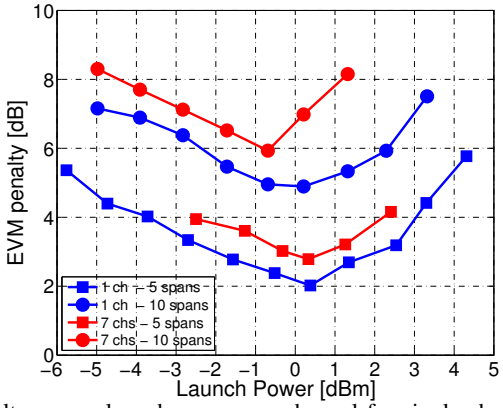

Fig. 9. EVM penalty versus launch power per channel for single channel and 7 channel transmission.

was set to 0 dB in order to operate the IQ-modulator at its quadrature point to achieve linearity. First, the optimum launch power was determined by varying the launch power whilst measuring the EVM as shown in Fig. 9. It was found to be approximately 0 dBm per channel except for WDM transmission over 800 km in which case it was found to be approximately -1 dBm.

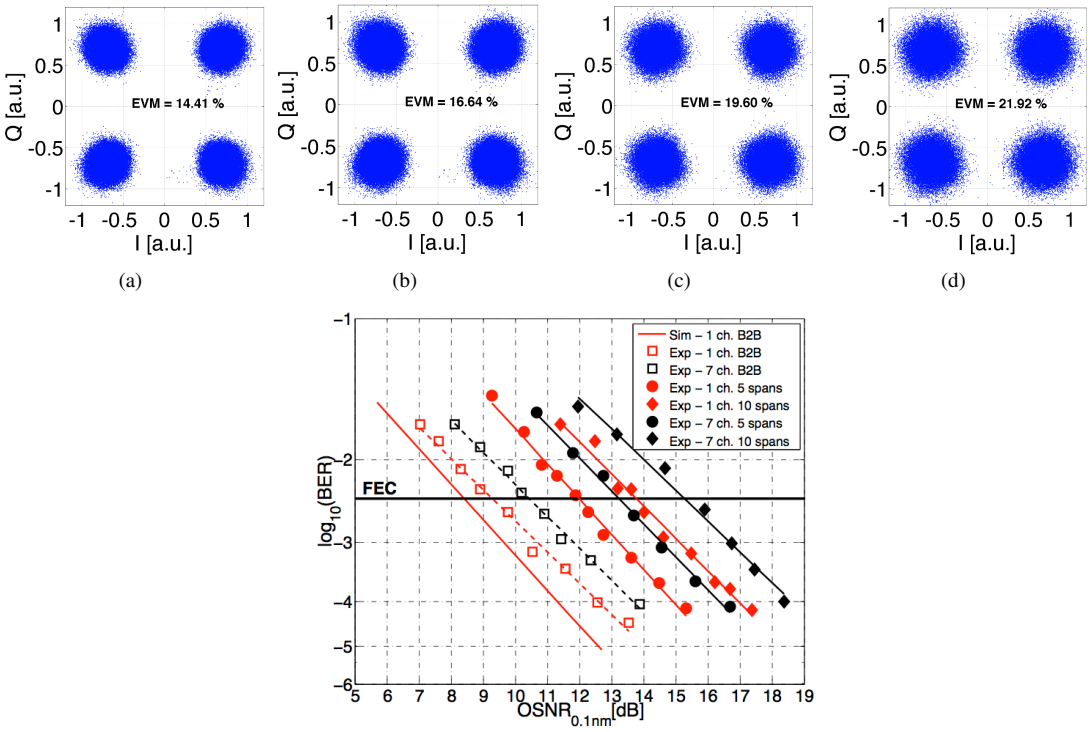

Fig. 10. Single ch. constellation after (a) 400 and (b) 800 km. 7 ch. constellation after (c) 400 km and (d) 800 km. (e) BER vs OSNR for back-to-back, 400 and 800 km for single and 7 channel transmission.

After the optimum launch power into the fiber was found, single channel and WDM transmission for targeted distances were performed. EVM gradually increases due to the crosstalk between the neighbouring channels and fiber nonlinearities which cause a gradual degradation

#201923 - $15.00 USD Received 28 Nov 2013; revised 6 Feb 2014; accepted 13 Mar 2014; published 11 Apr 2014

in receiver sensitivity as presented in Fig. 10(a)–10(e). The BER versus OSNR measurements for single channel and WDM transmission are plotted with the back-to-back measurements in Fig. 10(e). The required OSNR values corresponding to the BER values at the HD-FEC threshold are compared and discussed with ideal and practical simulation results below.

To demonstrate the fundamental limits of the system, simulations under ideal conditions were performed and the results are presented in Fig. 11(a). Additionally, to validate the experimental results, further (practical) simulations that incorporate the experimental parameters, *e.g.,* ENOB of DACs and limited bandwidth of electrical components at the transmitter/receiver, were also carried out and are shown in Fig. 11(b). The experimental results for both single channel and the WDM system matched well with the practical simulation results (see Fig. 11(b)). The required OSNR values for single channel transmission after 400 km of SSMF were 11.4, 11.8 and 12 dB for the ideal simulation, practical simulation and experiment, respectively. At 800 km, the corresponding OSNR values were 12.5, 13.2 and 13.8 dB. The penalty in single channel case between 400 and 800 km is due to the increase in PAPR resulted from EPD and self-phase modulation (SPM). The penalty can be improved through the use of higher resolution DACs.

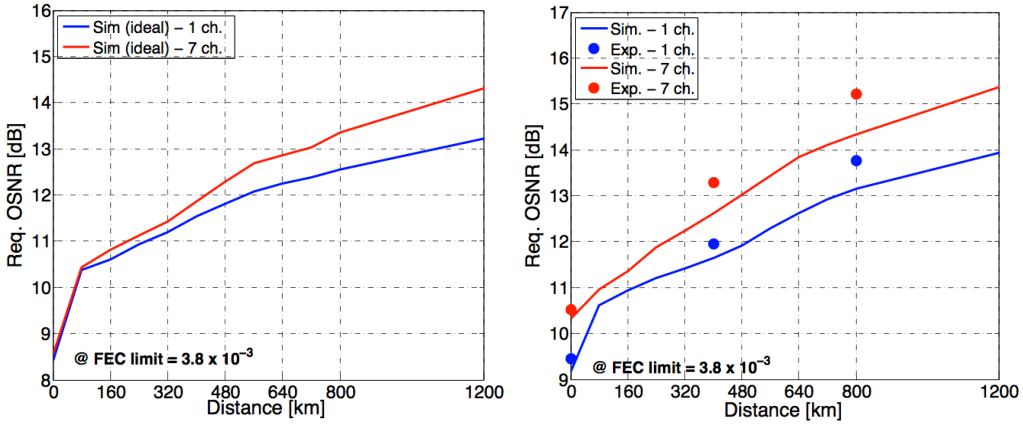

(a) (b)

Fig. 11. Required OSNR versus transmission distance (a) for the ideal simulations (b) comparison between experimental results and practical simulation results including DAC quantization noise, electrical bandwidth limitations in the transmitter/receiver, and 3rd-order super-Gaussian optical filter.

Furthermore, in WDM transmission over 400 km of SSMF, the corresponding required OSNR values were measured to be 11.9, 12.5 and 13.3 dB (see Fig. 10(e)). When the transmission distance increased to 800 km, the values at the HD-FEC threshold also increased to 13.4, 14.3 and 15.3 dB. This increase is due to four-wave mixing (FWM) caused by neighbouring channels. Over longer transmission distances, the required OSNR increases more rapidly in WDM transmission relative to the single channel transmission case due to fiber nonlinearity. During the single channel transmission, only SPM distorts the signal (the distortion exhibits a non-gaussian distribution around symbol points as shown in Fig. 10(a) and 10(b)) whereas FWM (gaussian distribution around the symbol points) between the closely spaced WDM channels degrades the system performance as shown in Fig. 10(c) and 10(d). Besides the nonlinear effects in optical fiber and chromatic dispersion, the non-optimal CSPR, used in the experiment in order to operate at the linear regime of the modulator is another factor that causes an additional OSNR penalty. This can be further optimized by employing pre-compensation for the modulator nonlinearity in the transmitter DSP, hence allowing the optimum CSPR to be used.

#201923 - $15.00 USD Received 28 Nov 2013; revised 6 Feb 2014; accepted 13 Mar 2014; published 11 Apr 2014

5. Conclusions

We investigated, for the first time, spectrally-efficient wavelength division multiplexed transmission of single-sideband QPSK SCM with Nyquist pulse shaping and electronic dispersion pre-compensation using direct detection. Operating at 14 Gb/s per channel and a channel spacing of 11 GHz, the system achieved a BER below a HD-FEC limit of 3.8×10^{-3} in transmission over SSMF fiber links of up to 800 km. The dispersion pre-compensation was performed digitally at the transmitter. A spectral efficiency of 1.2 b/s/Hz was demonstrated, taking into account a 7 % FEC overhead. Further increases in spectral efficiency could potentially be achieved with higher-order SSB QAM-SCM. This format offers a promising and cost-effective approach for spectrally-efficient metro, access and back-haul applications.

Acknowledgments

This work has been supported by the EU ERA-NET+ project PIANO+ IMPACT, EPSRC UNLOC EP/J017582/1 and EPSRC grant COSINE EP/I012702/1 and the authors thank Dr. S. J. Savory for stimulating discussions, M. Belmonte and Oclaro for providing the modulators, and Yenista Optics for the loan of the ultra-narrow bandwidth tunable filter.

#201923 - $15.00 USD Received 28 Nov 2013; revised 6 Feb 2014; accepted 13 Mar 2014; published 11 Apr 2014